2005 American Control Conference
June 8-10, 2005. Portland, OR, USA

A Voltage-Based Observer Design for Membrane Water Content in PEM Fuel Cells

Haluk Görgün* Murat Arcak† Frano Barbir*

*Connecticut Global Fuel Cell Center
44 Weaver Rd. Unit 5233, University of Connecticut
Storrs, CT 06269
{haluk,fbarbir}@engr.uconn.edu

†Department of Electrical, Computer, and Systems Engineering
110 8th Street, Rensselaer Polytechnic Institute
Troy, NY 12180
arcakm@rpi.edu

Abstract— **This paper presents a scheme for estimating membrane water content in polymer electrolyte membrane (PEM) fuel cells from voltage, current, temperature, and several pressure measurements. The approach is to exploit the resistive voltage drop which is closely associated with membrane water content. To distinguish this resistive drop from other voltage losses we make use of a well-developed fuel cell voltage model that characterizes each loss term, as well as the open circuit voltage. The unmeasured hydrogen and oxygen partial pressure values in the open-circuit model are estimated with a variant of the hydrogen and oxygen observers developed in [2]. Preliminary experimental results, obtained at the Connecticut Global Fuel Cell Center, are presented and discussed.**

I. Introduction

Polymer electrolyte membrane (PEM) fuel cells are envisioned to be the future choice for portable power, transportation, and combined heat and power, systems. They offer advantages to other fuel cell types, including relative simplicity of their design, and their ability to operate at low temperatures. A central problem in the operation of PEM fuel cells, however, is water management. The membrane must be sufficiently hydrated because its conductivity depends critically on the humidity level. Too little water causes membrane drying, which increases the ionic resistance, and exacerbates the voltage drop due to ohmic losses. Too much water causes "flooding", that is blocking of porous passages, which reduces the transport rate of reactants to the catalyst site.

An obstacle to active control of membrane water content is the lack of adequate tools for monitoring humidity in the fuel cell. The cost and size of existing humidity sensors are prohibitive for in-situ measurements. Their accuracy is also impaired for high relative humidity levels [11], at which a PEM fuel cell must operate. Other measurement techniques, such as [16] which employs gas chromatography, require extractive sampling and, thus, are slow and intrusive.

In this paper we present an estimation scheme for the membrane water content. Our idea is to first estimate the membrane resistance and, next, to use available characterizations of membrane resistance as a function of water content, such as those in [18] for Nafion 117 membranes. To accomplish the first step of membrane resistance estimation we calculate the ohmic voltage loss from voltage and current measurements, and from the well-developed fuel cell voltage model [14] which accounts for other voltage loss terms. Because the open-circuit voltage component of this model depends on partial pressures of hydrogen and oxygen, which are unavailable for measurement, we estimate them from a variant of the hydrogen and oxygen observers developed in [2]. We wish to emphasize that our estimation scheme is applicable when the current is nonzero, because it relies on the resistive voltage drop which is induced by the current.

A different approach to humidity estimation is presented in [15], where the authors employ open-loop observers based on lumped dynamic models for anode and cathode relative humidities. A significant contribution of [15] is to experimentally determine the diffusion coefficient in these dynamic models as

an affine function of relative humidity. This approach differs from our voltage-based estimation because, first, it does not make use of the voltage output of the humidity model and, second, it assumes open-circuit conditions. In contrast, we rely on the voltage output and its static relation to water content, and do not employ a dynamic humidity model. A combination of the two approaches would be possible once the model of [15] is extended to nonzero current conditions.

Due to the absence of humidity measurements in our set-up, in this paper we compare our membrane resistance estimates to ac resistance measurements. The results reveal an unmodeled effect of cell drying on *charge transfer resistance* [7]. Upon compensation for this effect, our resistance estimates match the measurements with reasonable accuracy.

The paper is organized as follows: In Section II we review the fuel cell voltage model and the characterization of membrane resistance as a function of its water content. The estimation algorithm is detailed in Section III, followed by experimental results and their interpretations in Section IV. Remaining research tasks and, in particular, a discussion of how the estimation design can be modified to account for flooding conditions, are presented in Section V.

II. Overview of the Voltage Model

The open-circuit voltage of a fuel cell is given by (see *e.g.* [14, Chapter 2]):

$$E = -\frac{\Delta\bar{g}_f^0}{2F} + \frac{RT}{2F}\left[\ln(p_{H_2}^{av}) + \frac{1}{2}\ln(p_{O_2}^{av})\right] \quad (1)$$

where $\Delta\bar{g}_f^0 < 0$ is the change in molar Gibbs free energy of formation at standard pressure, R is the universal gas constant, F is the Faraday constant, T is the cell temperature, $\ln(\cdot)$ denotes the natural logarithm, and $p_{H_2}^{av}$ and $p_{O_2}^{av}$ represent average values of hydrogen and oxygen partial pressures across the anode and cathode channels, respectively. As discussed in [2, Section III], a good approximation for these average values is the arithmetic mean of the inlet and exit partial pressures.

The operational voltage of the fuel cell differs from its open-circuit value, E, due to the *activation voltage drop*, V_a; the *ohmic voltage drop*, V_{ohm}; and the *mass transport loss*, V_{mass}, as detailed in [14, Chapter 3]. For a stack of n cells, the net voltage is thus:

$$V_{st} = n(E - V_a - V_{ohm} - V_{mass}). \quad (2)$$

The cumulative effect of the voltage loss terms in (2) is visible from the *polarization curve* in Figure 1, which plots the cell voltage as a function of the *current density*; that is, total current I divided by effective membrane area, A_m:

$$i = \frac{I}{A_m}. \quad (3)$$

Other voltage losses due to fuel crossover and internal currents [14, Section 3.5] are not included in (2) because their effect is considerable only at very low current densities.

The activation voltage drop is the voltage lost in driving the chemical reactions on the surface of the electrodes. It is given by the well-known empirical formula [14, Section 3.4]:

$$V_a = \frac{RT}{2\alpha F}\ln\left(\frac{i}{i_0}\right) \quad i > i_0, \quad (4)$$

where α is the *charge transfer coefficient*, and i_0 is the *exchange current density*, which depends on the temperature, pressure, the type of catalyst and its specific surface area and loading [10]. Likewise, the mass transfer voltage drop is given by [14, Section 3.7]:

$$V_{mass} = -B\ln\left(1 - \frac{i}{i_{lim}}\right), \quad (5)$$

where i_{lim} is the *limiting current density*, and B is a constant that depends on the fuel cell, and its operating conditions.

Finally, the ohmic voltage drop is

$$V_{ohm} = (R_m + r)I, \quad (6)$$

where R_m is the membrane resistance, and r represents the sum of other components, such as resistance through electrically conductive components of the fuel cell, including contact resistance, and resistance from the electrodes. Because measurement techniques are available to distinguish between the components of total resistance [17], for our design in the next section we assume that r is known.

The membrane resistance, R_m, depends critically on the membrane *water content*, which is defined as the ratio of the number of water molecules to the number of charge sites. Indeed, as shown in [18], water content affects the membrane resistance via

$$R_m = \frac{t_m}{A_m(0.00514\lambda_m - 0.00326)}\exp\left[1268\left(\frac{1}{T} - \frac{1}{303}\right)\right] \quad (7)$$

where t_m and A_m are the membrane thickness, and area, respectively. The study in [18] also relates the water content to the membrane *relative humidity*, ϕ_m, (the ratio of water partial pressure to saturated vapor pressure) by the empirical formula:

$$\lambda_m = 0.043 + 17.81\phi_m - 39.85\phi_m^2 + 36.0\phi_m^3. \quad (8)$$

III. Estimation of Water Content

To estimate the water content, λ_m, our approach is to first estimate R_m and, next, to invert the function (7) to obtain the estimate $\hat{\lambda}_m$. For the estimation of R_m we rely on (6), in which I is available for measurement and r is known. Because V_{ohm} is not measured separately, it is to be calculated from the measurement of the net voltage V_{st}, by substituting in (2) the values of E, V_a, and V_{mass}, calculated from (1), (4), and (5), respectively.

This algorithm is not to be applied for zero or small values of the current I, because the computation of R_m from (6) involves division by I. It is reliable when the fuel cell operates in the linear region of the polarization curve because, then, the effect of humidity on the open-circuit voltage, not modeled in (1), and losses due to fuel crossover and internal currents, not accounted for in (2), are indeed negligible compared to the ohmic voltage drop. Since the linear region of the polarization curve is the desired regime of fuel cell operation, this restriction does not impair the practical relevance of our algorithm.

The main difficulty in this algorithm is the calculation of the open-circuit voltage, E, from (1), which relies on the unmeasured hydrogen and oxygen partial pressures, $p_{H_2}^{av}$ and $p_{O_2}^{av}$. To overcome this difficulty we employ a variant of the hydrogen and oxygen observers developed in [2]. To this end we denote by p_{H_2} the exit partial pressure of hydrogen in the anode channel and obtain, from the Ideal Gas Law, the lumped dynamic model:

$$\dot{p}_{H_2} = \frac{RT}{Vol_a}\left(\frac{1}{M_{ai}}\frac{p_{H_{2in}}}{P_{ain}}F_{ai} - \frac{1}{M_{ao}}\frac{p_{H_2}}{P_a}F_{ao} - \frac{nI}{2F}\right) \quad (9)$$

where Vol_a is the anode volume, P_a is the total anode pressure, $p_{H_{2in}}$ and P_{ain} are, respectively, the hydrogen partial pressure and the total pressure at the inlet of the anode, F_{ai} and F_{ao} are the total inlet and outlet mass flows, and M_{ai} and M_{ao} represent average molecular weights of the inlet and exit gas streams. The bracketed expression in (9) calculates the molar rate of change of hydrogen. In particular, the first term represents the increase in hydrogen mole number due to the inlet flow, the second term is the decrease due to the exit flow, and the third term is the consumption due to the fuel cell reaction.

For observer design we assume that the total pressures P_{ain} and P_a, and the mass flows F_{ai} and F_{ao}, are known. The mass flows can either be measured with flowmeters, or estimated from pressure differences via orifice equations, such as those used in [2]. The variables M_{ai} and $p_{H_{2in}}$ which appear in the coefficient of F_{ai} in (9) are also assumed to be available. This assumption is meaningful when the gas composition of the inlet stream is known, or estimated with a separate observer for the fuel reformer as in [12]. Our observer is

$$\dot{\hat{p}}_{H_2} = \frac{RT}{Vol_a}\left(\frac{1}{M_{ai}}\frac{p_{H_{2in}}}{P_{ain}}F_{ai} - \frac{1}{\hat{M}_{ao}}\frac{\hat{p}_{H_2}}{P_a}F_{ao} - \frac{nI}{2F}\right) \quad (10)$$

where, for the unknown M_{ao}, we employ the value

$$\hat{M}_{ao} = \frac{\hat{p}_{H_2}}{P_a}M_{H_2} + \frac{P_a - \hat{p}_{H_2}}{P_a}\delta_a, \quad (11)$$

in which M_{H_2} is the molecular weight of hydrogen, and δ_a is an average value for the molecular weights of other gases at the anode exit. Unlike the design in [2] which employed a constant average value for $\hat{M}_{ao}$, the new observer (10)-(11) is nonlinear in $\hat{p}_{H_2}$ due to the dependence of $\hat{M}_{ao}$ on $\hat{p}_{H_2}$. However, because hydrogen is lighter than the other molecules; that is, $M_{H_2} < \delta_a$ in (11), the right-hand side of (10) is a monotone decreasing function of $\hat{p}_{H_2}$, which guarantees observer convergence as proven in [3].

Using a similar model for the cathode, we obtain the oxygen observer

$$\dot{\hat{p}}_{O_2} = \frac{RT}{Vol_c}\left(\frac{1}{M_{ci}}\frac{p_{O_{2in}}}{P_{cin}}F_{ci} - \frac{1}{\hat{M}_{co}}\frac{\hat{p}_{O_2}}{P_c}F_{co} - \frac{nI}{4F}\right) \quad (12)$$

$$\hat{M}_{co} = \frac{\hat{p}_{O_2}}{P_c}M_{O_2} + \frac{P_c - \hat{p}_{O_2}}{P_c}\delta_c\,, \quad (13)$$

where Vol_c is the cathode volume, P_c is the total cathode pressure, $p_{O_{2in}}$ and P_{cin} are the oxygen partial pressure and the total pressure at the inlet of the cathode, F_{ci} and F_{co} are the total inlet and outlet mass flows, M_{ci} and M_{co} represent average molecular weights of the inlet and exit gas streams, M_{O_2} is the molecular weight of oxygen, and δ_c is an average value for the molecular weights of other gases in the exit stream.

Thus, to estimate the membrane water content λ_m, we first estimate the open-circuit voltage E by obtaining $\hat{p}_{H_2}$ and $\hat{p}_{O_2}$ from the observers (10)-(11) and (12)-(13), and by substituting in (1) the average values:

$$p_{H_2}^{av} = \frac{\hat{p}_{H_2} + p_{H_{2in}}}{2} \qquad p_{O_2}^{av} = \frac{\hat{p}_{O_2} + p_{O_{2in}}}{2}. \quad (14)$$

Next, we calculate V_{ohm} from (2), using our estimate of E, as well as the measurement of voltage V_{st}, and the calculation of V_a and V_{mass} from (4)-(5). We then obtain the membrane resistance estimate $\hat{R}_m$ from (6) by using the current measurement I, and by subtracting r. Finally, we use this $\hat{R}_m$ to estimate the water content $\hat{\lambda}_m$ from (7), and obtain $\hat{\phi}_m$ from the unique real root of the polynomial (8), given by:

$$\hat{\phi}_m = 0.369 + (S + \sqrt{Q^3 + S^2})^{1/3} + (S - \sqrt{Q^3 + S^2})^{1/3} \quad (15)$$

where $S = -0.0416 + \hat{\lambda}_m/72$ and $Q = 0.0288$.

IV. Experimental Results

We now present preliminary experimental results for the algorithm developed in the previous section. These experiments have been performed at the Connecticut Global Fuel Cell Center, with a fuel cell developed and manufactured by Proton Energy Systems. The stack consists of $n = 3$ cells, with $A_m = 65$ cm^2 active area each, and with $t_m = 0.0051$ cm thickness. The cathode flow field consists of six parallel channels in serpentine layout, while the anode flow field has a single serpentine channel. The channels are rectangular with 0.8 mm width and depth. The stack is air-cooled. Hydrogen is supplied by a HOGEN 40 electrolyzer, built by Proton Energy Systems, and air is supplied from air cylinders. Hydrogen and air flows are regulated by a Lynntech FCTS GMET/H Gas Metering System. A Lynntech Gas Humidifier, FCTS H0101, achieves the desired humidification of the reactant gases before entering the fuel cell stack by controlling the humidification temperature. The cell resistance is measured by an Agilent 4338B Milliohmmeter. A Lynntech FCTS I/O box is used to collect the measured data in the test platform. A TDI RBL 488 electronic load bank is used to generate the load current profile.

We first compare the voltage model of Section II to the experimental polarization curve. To obtain this curve we set the hydrogen flow rate to 1 slpm (standard liter per minute), and the air flow rate to 3 slpm. The hydrogen and air humidification temperatures were set to 60°C. To prevent condensation, we set the line-heaters for hydrogen and oxygen to 70°C. We observed the open circuit voltage for each cell, then gradually increased the current up to 25 A, and reduced it back to zero. The resulting curve is given in Figure 1, where the discrete data points are obtained from step changes in the current. We obtained a close match to these data points using the voltage model of Section II (continuous curve in Figure 1) with $B = RT/(2F)$ and $i_{lim} = 0.4$ A/cm^2 in (5), $\alpha = 0.5$ in (4), and with i_0 obtained from a temperature- and pressure-dependent formula in [10], in which we used the reference value $i_0^{ref} = 8.78 \cdot 10^{-11}$ A/cm^2.

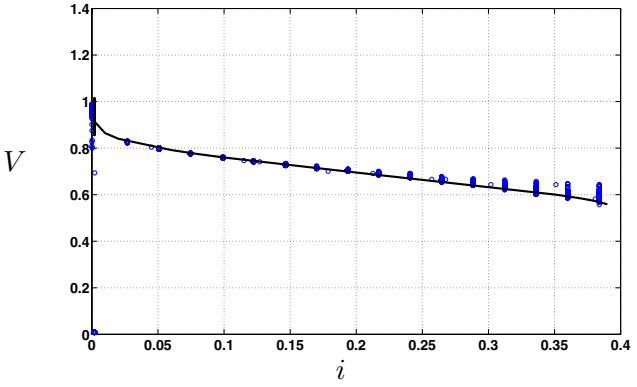

Fig. 1. Voltage of a single cell (Volts) versus current density i (A/cm^2). The voltage model of Section II (continuous curve) matches the discrete data points.

To test our humidity estimation algorithm, we induced membrane drying by reducing the air inlet humidification temperature below the cell temperature. This causes the air to absorb membrane humidity as it passes through the warmer cell. The resulting increase in the resistance and the decrease in the cell voltage are shown in Figure 2 for a current of 20 A. Due to the absence of humidity measurements in our set-up, in this paper we only compare our estimate $\hat{R}_m$ for the membrane resistance to that obtained from the ac resistance measurement in Figure 2, performed at 1 kHz. The observer calculations are presently carried out off-line, from filtered experimental data.

At fully humidified conditions the cell performance was in steady state and the ac resistance measurement indicated 4.3 mΩ (280 mΩcm^2), as shown in Figure 2. The model (7) predicts the membrane resistance to be $R_m = 0.78$ mΩ (51 mΩcm^2), which means $r = 4.3 - 0.78 = 3.52$ mΩ (228 mΩcm^2). 10 mΩcm^2 of this may be attributed to the resistance from the

electrodes [8]. Therefore, the electronic resistance is $218\ \mathrm{m\Omega cm^2}$, which includes the resistance through the electrically conductive components of the fuel cell. In [4], the electronic resistance is reported to be up to 3 times larger than the ionic resistance (membrane and electrodes). This, of course, depends on the cell design.

Under drying, the cell resistance increased at a rate of $0.0018\ \mathrm{m/s}$. The electronic resistance should be fairly independent of the drying conditions i.e., membrane water content. Although drying of a membrane results in reduced membrane thickness, in a well designed fuel cell stack, the changes in the membrane thickness should be compensated by a stack compression mechanism. In case of the Proton Energy System's stack this compression is accomplished with five polyurethane springs distributed evenly over the center of the active area [9].

It is therefore safe to assume that only the ionic resistance changes with humidity in the cell. However, the resulting observer estimate of R_m derived from the observance of the cell stack potential, upon addition of $r = 3.52\ \mathrm{m\Omega}$, (dotted curve in Figure 2) does not match the cell resistance change. In fact, ac resistance measurements showed that only 40% of the increase in voltage loss due to drying is from the increase in ohmic resistance. This indicates that there are other factors affecting the cell potential under drying conditions. Indeed, it is reported in [1] that drying of the anode catalyst layer not only increased the membrane proton-conduction resistance but also increased the activation overpotential for the hydrogen oxidation reaction due to a decrease in the number of active sites on the anode side. A similar argument may be applied to the cathode drying scenario in our experiment.

To compensate for this loss of catalytic activity, which may be modeled as an increase in activation overpotential, in our estimator computations we relied on our empirical observation and calculated 40% of the increase in voltage loss to be due to the increase in $\hat{R}_m$. The resulting observer estimate $\hat{R}_m$, plotted in Figure 2 with a dashed-line upon addition of $r = 3.52$ $\mathrm{m\Omega}$, matches the experimentally determined increase in cell resistance with reasonable accuracy.

Using this $\hat{R}_m$ we obtain from equations (7) and (15) the estimates, $\hat{\lambda}_m$ and $\hat{\phi}_m$, as in Figure 3. It is clear that the membrane was intensively drying with $\hat{\lambda}_m$ dropping below 4. The conditions in the cell changed from fully humidified ($T_{hum} = 75°\mathrm{C}$, $T_{cell} = 70°\mathrm{C}$) to dry ($T_{hum} = 45°\mathrm{C}$, $T_{cell} = 65°\mathrm{C}$). At dry conditions, the air at the exit of the stack had relative humidity of 85% (calculated from the stack mass balance), taking into account the product water added to the air stream.

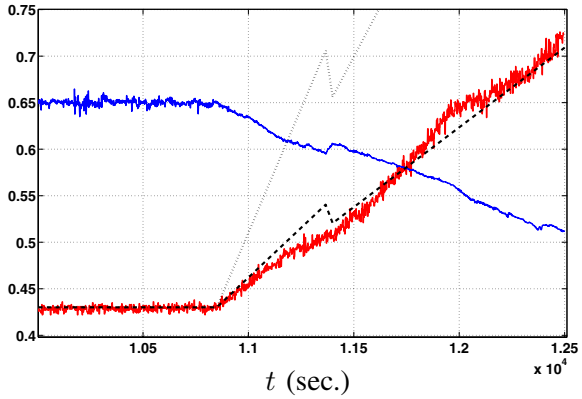

Fig. 2. Voltage decrease and resistance ($\Omega \cdot 10^{-2}$) increase in response to drying, which starts at $t = 10850$ sec. The dotted line is the sum of our estimate $\hat{R}_m$, and $r = 3.52$ $\mathrm{m\Omega}$, before compensation for the loss of catalytic activity. The dashed line, obtained upon compensation, is closer to the ac resistance measurement.

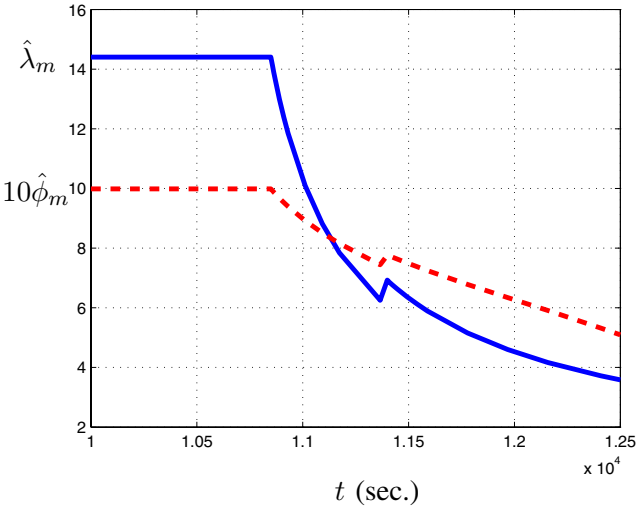

Fig. 3. Water content estimate $\hat{\lambda}_m$, and relative humidity estimate $\hat{\phi}_m$, scaled by 10, obtained via equations (7) and (15) from the estimate $\hat{R}_m$ in Figure 2.

V. Conclusions

Water management is one of the most critical problems in PEM fuel cell operation. In this paper a method for estimation of membrane water content has

been developed by exploiting its effect on cell resistive voltage drop. This method relies on measurements of voltage, current, temperature, and total pressure in the anode and cathode. It also incorporates observers for hydrogen and oxygen partial pressures adapted from [2].

A voltage drop at constant current may also be caused by flooding - an effect completely opposite from drying. In order to avoid an incorrect attribution of this voltage drop to drying, a cathode pressure drop may be monitored [5] and used in control algorithm. Pressure drop on the cathode side increases with cell flooding, while it remains unchanged with cell drying, thus clearly distinguishing between the two phenomena [6], [13], [5].

Dry conditions at the cell inlet and outlet mean that all of the water generated in the electrochemical reaction evaporated, unlike in steady state saturated conditions at cathode inlet and outlet when all of the product water left the stack as liquid. The Gibbs free energy, and therefore the theoretical cell potential, are lower for gaseous product water. Additional effects of water evaporation on local temperature, and therefore on saturation conditions, may only be determined by detailed 3-D modeling, and then integrated over the entire cell.

A significant effect of cell drying on activation overpotential, i.e., charge transfer resistance, has been detected. Further modeling efforts will attempt to establish a functional relationship between the membrane water content and activation overpotential.

Acknowledgement. The authors would like to thank Dr. Alevtina Smirnova of the Connecticut Global Fuel Cell Center for her help in interpreting experimental results. The work of the second author is supported by NSF under grant ECS-0238268.

REFERENCES

[1] B. Andreaus, A.J. McEvoy, and G.G. Scherer. Analysis of performance losses in polymer electrolyte fuel cells at high current densities by impedance spectroscopy. *Electrochimica Acta*, 47:2223–2229, 2002.

[2] M. Arcak, H. Gorgun, L.M. Pedersen, and S. Varigonda. A nonlinear observer design for fuel cell hydrogen estimation. *IEEE Transactions on Control Systems Technology*, 12(1):101–110, 2004.

[3] M. Arcak and P. Kokotović. Nonlinear observers: A circle criterion design and robustness analysis. *Automatica*, 37(12):1923–1930, 2001.

[4] F. Barbir, J. Braun, and J. Neutzler. Effect of collector plate resistance on fuel cell stack performance. In S. Gottesfeld and T.F. Fuller, editors, *Proton Conduction Membrane Fuel Cells II*, volume 98-27, pages 400–406. The Electrochemical Society, Pennington, NJ, 1999.

[5] F. Barbir, H. Gorgun, and X. Wang. Relationship between pressure drop and cell resistance as a diagnostic tool for PEM fuel cells. Accepted for publication in *Journal of Power Sources*, 2004.

[6] F. Barbir, A. Husar, and V. Venkataraman. Pressure drop as a diagnostic tool for PEM fuel cells. In *The 2001 Electrochemical Society Meeting*, San Francisco, CA, 2001.

[7] A.J. Bard and L.R. Faulkner. *Electrochemical Methods: Fundamentals and Applications*. Wiley, second edition, 2001.

[8] F.N. Buchi and G.G. Scherer. Investigation of the transversal water profile in nafion membranes in polymer electrolyte fuel cell. *Journal of the Electrochemical Society*, 148(3):A183–A188, 2001.

[9] O. Chow, J. Friedman, D. Halter, and F. Barbir. Evaluation of a novel design air-cooled 1 kw PEM-based fuel cell stack. In *1st International Conference on Fuel Cell Development and Deployment*, Storrs, CT, 2004.

[10] H.A. Gasteiger, W. Gu, R. Makharia, and M.F. Mathias. Tutorial: catalyst utilization and mass transfer limitations in the polymer electrolyte fuel cell. In *The 2003 Electrochemical Society Meeting*, Orlando, FL, 2003.

[11] R.S. Glass, editor. *Sensor Needs and Requirements for Proton-Exchange Membrane Fuel Cell Systems and Direct-Injection Engines*. Lawrence Livermore National Laboratory, Applied Energy Technologies Program, Livermore, California, 2000.

[12] H. Gorgun, M. Arcak, S. Varigonda, and S. Bortoff. Nonlinear observer design for fuel processing reactors in fuel cell power systems. In *Proceedings of the 2004 American Control Conference*, pages 845–849, Boston, MA, 2004.

[13] W. He, G. Lin, and T.V. Nguyen. Diagnostic tool to detect electrode flooding in proton exchange membrane fuel cells. *AIChE Journal*, 49(12):3221–3228, 2003.

[14] J. Larminie and A. Dicks. *Fuel Cell Systems Explained*. John Wiley & Sons, Inc., Chicester, second edition, 2003.

[15] D. McKay and A. Stefanopoulou. Parametrization and validation of a lumped parameter diffusion model for fuel cell stack membrane humidity estimation. In *Proceedings of the 2004 American Control Conference*, pages 816–821, Boston, MA, 2004.

[16] M.M. Mench, Q.L. Dong, and C.Y. Wang. In-situ water distribution measurements in a polymer electrolyte fuel cell. *Journal of Power Sources*, 124:90–98, 2003.

[17] M. Smith, D. Johnson, and L. Scribner. Electrical test methods for evaluating fuel cell MEA resistance. *Fuel Cell Magazine*, pages 15–17, February/March 2004.

[18] T.E. Springer, T.A. Zawodzinski, and S. Gottesfeld. Polymer electrolyte fuel cell model. *Journal of Electrochemical Society*, 138(8):2334–2342, 1991.